Colloid Polym Sci (2004) 283: 306–316
DOI 10.1007/s00396-004-1144-x

ORIGINAL CONTRIBUTION

Keita Suzuki
Jun-ichi Oku
Kenichi Izawa
Hiro-Fumi Okabayashi
Isao Noda
Charmian J. O'Connor

Two-dimensional correlation gel permeation chromatography (2D GPC) study of the CH_3SO_3H-catalyzed polymerization of triethoxysilyl-terminated polystyrene. Molecular weight effect on the aggregate–aggregate interactions

Received: 24 January 2004
Accepted: 2 March 2004
Published online: 4 August 2004

K. Suzuki · J. Oku · H.-F. Okabayashi (✉)
Department of Applied Chemistry,
Nagoya Institute of Technology,
Gokiso-cho, Showa-ku, Aichi 466–8555
Nagoya, Japan
E-mail: fwiw4348@mb.infoweb.ne.jp

K. Izawa
Chromato Dept., Fuji Silysia Chemical
Ltd., 1846 Kozoji2, 487–0013
Kasugai, Aichi, Japan

I. Noda
The Procter and Gamble Company,
8611 Beckett Road, West Chester, OH
45069, USA

C. J. O'Connor
Department of Chemistry,
The University of Auckland,
Private Bag 92019, Auckland,
New Zealand

Abstract The two-step polymerization process of two well-defined polymeric silane coupling agents, triethoxysilyl-terminated polystyrene with molecular weights equal to 2400 [TESi-PS (2400)] and 8000 [TESi-PS (8000)], catalyzed by 0.1 mol/kg CH_3SO_3H, was traced as a function of reaction time using gel-permeation chromatography (GPC). Two sets of GPC traces, collected during the condensation, were then converted to two-dimensional (2D) correlation spectra by using generalized 2D correlation theory. The 2D correlation spectra elucidated details of the aggregate–aggregate correlations [in particular, the difference between the correlations of TESi-PS (2400) and TESi-PS (8000)], thus demonstrating the effect of aggregation on the polymerization.

Keywords Two-dimensional correlation gel permeation chromatography · Aggregate · Molecular weight · Triethoxysilyl-terminated polystyrene · CH_3SO_3H-catalyzed polymerization

Introduction

A novel analytical method, two-dimensional correlation gel permeation chromatography (2D GPC), in which generalized 2D correlation theory [1, 2, 3] was combined with time-resolved GPC, was first introduced by Izawa et al. [4, 5, 6, 7, 8]. It has been demonstrated that this technique can be used effectively to study the intricate details of polymerization processes. For example, Izawa et al. [6, 7, 8] traced the HCl-catalyzed sol–gel polymerization of relatively simple silane coupling agents (SCAs), and particularly that of perfluorooctyl- and *n*-octyl-triethoxysilane, as a function of reaction time using the conventional GPC technique. A set of GPC traces, collected sequentially at different sampling times during the condensation reaction, were then converted to 2D correlation spectra. It was found that 2D GPC correlation spectra thus obtained directly reflected the mechanism of the polymerization process. However, since the molecular weights of the polymeric precursors, formed during the polymerization of these SCAs, were relatively low, it was difficult to use polystyrene calibration curves to determine precisely the degree of polymerization of

each condensate. This absence of critical information limited any meaningful in-depth discussion of the intricate details of the aggregate–aggregate interactions during polymerization.

Recently, Suzuki et al. [9, 10, 11] reported details of the acid-catalyzed condensation reaction of five well-defined polymeric SCAs, triethoxysilyl-terminated polystyrenes (TESi-PSs), substituted with various polystyrene moieties of high molecular weights. The use of polymeric SCAs made the accurate determination of the degree of polymerization of each product possible by using a relevant polystyrene calibration curve. Furthermore, the combined effects on the reaction rate of the molecular weight of TESi-PS, the amount of included polystyrene, and the use of nonpolar solvents were examined in detail [12]. The kinetic data provided irrefutable evidence that the formation of aggregates during the polymerization process accelerates the reaction rate. This acceleration effect was accounted for by postulating an aggregation model in which the ethoxysilyl groups were concentrated in the polar core. Support for this model comes from the fact that the polymeric alkoxy moiety of a polymeric SCA tends to form an aggregate in organic solvents [13, 14, 15].

Recently, Ogasawara et al. [16] examined the polymerization of *n*-octyl-triethoxysilane (OTES) in ethanol by using time-resolved small-angle X-ray scattering (SAXS). They showed that this polymerization consists of two separate steps: a monomer–monomer and a cluster–cluster growth process. Significantly, the second step, which may be regarded as a transition in the building of a macroscopic structure, occurs well before the final macroscopic phase transition. Furthermore, Izawa et al. [17] used SAXS spectra to detect the aggregates of OTES and perfluoro-octyl-triethoxysilane (PFOTES) in ethanol as a polar solvent. The time-resolved SAXS profiles led to the postulation of an aggregational model. It was proposed that condensation between SiOH groups results in a particle with an internal Si–O–Si bonding network structure, which expands to form the core of a particle with external hydrophobic chains. This model is therefore very similar to that of a reversed micelle.

It is thus of interest to examine the mechanism of polymerization of a polymeric SCA, such as TESi-PS, by using time-resolved GPC combined with 2D correlation analysis, to elucidate further the intricacies of the process. In this study, the time-resolved GPC elution profiles of two polymeric SCAs, TESi-PS samples with molecular weights equal to 2,400 [TESi-PS (2400)] and 8,000 [TESi-PS (8000)] respectively, were used to calculate the 2D correlation spectra. In particular, the difference between the polymerization process of the two TESi-PSs has been examined and the effect of aggregation of high molecular weight TESi-PS, on the reaction mechanism has been presented.

Background

The time-resolved GPC trace intensity $I(E, t)$ can be expressed as a function not only of the chromatographic elution time E but also of the sampling time t for each aliquot collected during a polymerization reaction period between $T_{\min}$ and $T_{\max}$. The dynamic GPC trace intensity $\tilde{y}(E,t)$ of the time-resolved GPC profile is given by

$$\tilde{y}(E,t) = \begin{cases} I(E,t) - \tilde{I}(E) & \text{for } T_{\min} \leqslant t \leqslant T_{\max} \\ 0 & \text{otherwise} \end{cases} \quad (1)$$

where $\tilde{I}(E)$ is the reference GPC trace profile of the reaction system. The reference trace $\tilde{I}(E)$ is set to be the time-average of trace profiles over the observed reaction period given by

$$\tilde{I}(E) = \frac{1}{T_{\max} - T_{\min}} \int_{T_{\min}}^{T_{\max}} I(E,t)\mathrm{d}t. \quad (2)$$

The generalized 2D correlation function for the analysis of time-resolved GPC profiles is defined as

$$\Phi(E_1,E_2) + i\Psi(E_1,E_2) = \frac{1}{\pi(T_{\max} - T_{\min})} \int_0^{\infty} \widetilde{Y_1}(\omega) \cdot \widetilde{Y_2}^*(\omega)\mathrm{d}\omega. \quad (3)$$

The real and imaginary terms, Φ (E_1, E_2) and Ψ (E_1, E_2), are the synchronous and asynchronous 2D correlation intensities, respectively. The synchronous 2D correlation intensity Φ (E_1, E_2) represents the overall similarity or coincidental trends between two separate intensity variations of the GPC trace measured at different elution counts. The asynchronous 2D correlation intensity Ψ (E_1, E_2), on the other hand, can be regarded as a measure of dissimilarity or out-of-phase character of the GPC trace intensity variations.

The term $\widetilde{Y_1}(\omega)$ is the forward Fourier transform of the dynamic trace intensity variations $\tilde{y}(E_1,t)$ observed at a specific elution count E_1 with respect to the sampling time t.

$$\widetilde{Y_1}(\omega) = \int_{-\infty}^{\infty} \tilde{y}(E_1,t)e^{-i\omega t}dt. \quad (4)$$

The conjugate Fourier transform, $\widetilde{Y_2}^*(\omega)$, of the GPC trace intensity variation $\tilde{y}(E_2,t)$, observed at elution time E_2 is given by

$$\widetilde{Y_2}^*(\omega) = \int_{-\infty}^{\infty} \tilde{y}(E_2,t)e^{+i\omega t}\mathrm{d}t. \quad (5)$$

While Fourier transformation of the dynamic trace $\tilde{y}(E,t)$, defined in Eq. 1, with respect to the sampling time t, formally provides the synchronous and asynchronous correlation spectra, Φ (E_1, E_2) and Ψ (E_1, E_2),

a simpler computational method has recently been developed to obtain Φ (E_1, E_2) and Ψ (E_1, E_2) more directly. Further details of synchronous and asynchronous 2D GPC spectra are described elsewhere [5, 6, 7, 8].

Materials and methods

Materials and condensation Living polystyrenes (PSs) with molecular weight (M_n) equal to 2,200 and 7,800 were prepared by anionic polymerization of styrene [18]. TESi-PSs with M_n equal to 2,400 and 8,000 were prepared by the coupling reaction of living PS and chlorotriethoxysilane [18]. The TESi-PS (2400) and TESi-PS (8000) thus obtained by recrystallization in methanol and drying in vacuum at circa 298 K, were used for condensation. Samples of the TESi-PS (40 mmol/kg), catalyst (CH_3SO_3H, 0.1 mol/kg) and tetrahydrofuran (THF) system were placed into each ampoule, sealed under high vacuum (10^{-3} mm Hg), and the contents homogenized by shaking. Condensation of TESi-PS in each reaction mixture was carried out in a temperature-controlled bath (333 K) for a prescribed time. The condensation was quenched by pouring the reaction mixture into a large excess of methanol, and the resulting TESi-PS polymer, which precipitated from each reaction mixture, was filtered through a glass filter and dried at circa 298 K.

Time-resolved GPC measurements GPC measurements were carried out by using a Toso HLC-802UR [G2000H and G3000H columns for TESi-PS (2400)] and a Toso HLC-802A [with two GMH columns for TESi-PS (8000)], each equipped with a refractive index (*RI*) detector and using a column oven temperature of 313 K. THF was used as the eluent. The nominal flow rate of the eluent was 1 mL/min. Actual flow rates were inspected during the recording of a GPC curve, and their constancy was confirmed in order to ensure that irreversible adsorption of insoluble polymer on the GPC column, which would have changed the flow rate, did not occur during the GPC measurements. The errors of an elution count were ± 0.1 min. The GPC data were calibrated with PS standards (Fig. 1). The signal-to-noise (S/N) ratios of the elution peaks and of the baseline, in the conventional GPC profiles, were checked to prevent error in the interpretation of the 2D GPC spectra. The averaged S/N ratios were 170. The amount of TESi-PS–catalyst–THF solution injected into the GPC column was controlled to provide a linearly increasing *RI* and a linearly increasing UV absorbance (at 360 nm), both parameters being measured simultaneously.

2D GPC correlation analysis Synchronous and asynchronous 2D GPC correlation spectra were calculated from the time-resolved GPC profiles. Calculations were carried out using the 2D OGAIZA software, which had been developed at the Nagoya Institute of Technology.

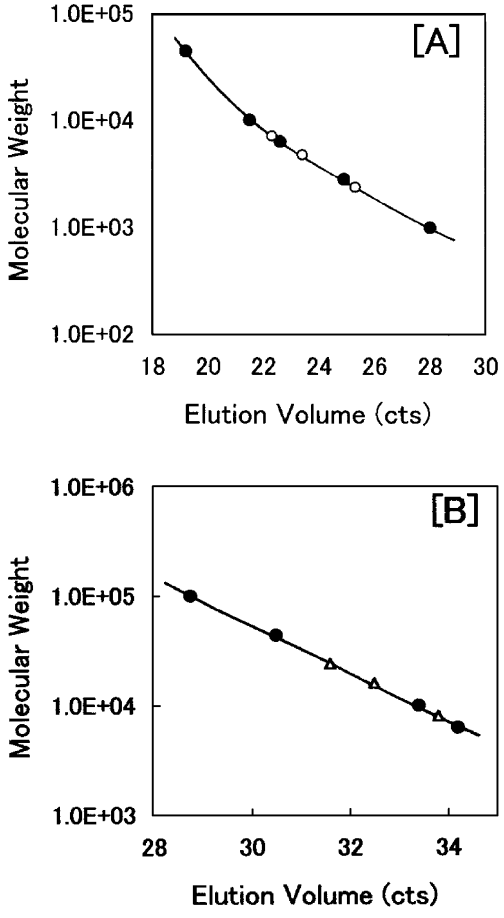

Fig. 1[A],[B] Calibration curves of polystyrene standards. **[A]** Triethoxysilyl-terminated polystyrene with molecular weights equal to 2400 [TESi-PS (2400)]. *Black circles* standards. *white circles* isolated polymers of TESi-PS (2400). **[B]** TESi-PS (8000). *Black circles* standards, *triangles* isolated polymers of TESi-PS (8000)

Results and discussion

In our previous papers [9, 10, 11, 12], we have reported data for the condensation reaction of TESi-PS, with a narrow molecular weight distribution ($M_w/M_n = 1.07$) and high functionality ($f > 96\%$), catalyzed by acid in various solvents, and, in particular, for the aggregational effects on the rate of condensation of TESi-PS [12]. The results showed that the rate of reaction strongly depends not only upon the species of the catalyst and solvent used for the condensation but also upon the molecular weight of the TESi-PS monomer. Results of special relevance to the present study may be summarized as follows.

The time course of the CH_3SO_3H-catalyzed condensation reaction for two TESi-PS monomers with

$M_n = 2{,}000$ and 8,600 yielded rate constants of $k \times 10^6\ s^{-1} = 110.1$ and $k \times 10^6\ s^{-1} = 724.5$, respectively, thus confirming that the higher molecular weight TESi-PS monomer condensed more rapidly. We present the following explanation for this observation. During the polymerization reaction, TESi-PS aggregates may be formed. As the M_n value of a PS moiety increases, the hydrophobicity of this portion becomes greater, promoting formation of aggregates with a core in which unhydrolyzed ethoxy groups are concentrated, thus leading to a faster reaction rate.

Application of the generalized 2D correlation analysis [1, 2] to the time-dependent GPC elution profiles of the CH_3SO_3H-catalyzed TESi-PS (2400)–THF and TESi-PS (8000)–THF systems made it possible to elucidate the difference in the polymerization mechanism arising from the difference in the M_n values of the two samples. Figure 2 shows the time-resolved GPC profiles, obtained at the same prescribed times, for the two systems. Tentative assignment of the elution peaks, based on the calibration with PS standards, is listed in Table 1. It is found that predominant production of the trimer of TESi-PS (8000) occurs more rapidly (at 2 h) than that of TESi-PS (2400) (at 4 h).

2D correlation GPC

The synchronous and asynchronous 2D GPC correlation spectra for the TESi-PS (2400) and TESi-PS (8000) systems, calculated directly from the two sets of time-dependent GPC profiles (Fig. 2), are shown in Fig. 3, Fig. 4, Fig. 5 and Fig. 6. The possible synchronous correlation squares (CSq_i, where $i = 1-5$) and their corresponding band correlations, are listed in Table 2. Band correlations, signs and orders of events are listed in Table 3.

TESi-PS (2400)

In the synchronous map (step I) of TESi-PS (2400) (Fig. 3a), the very strong intensity of autopeak A at 25.5 min and the medium intensity of autopeak B at 23.2 min suggest that the monomers (band A) are rapidly consumed to produce dimers (band B). The strong negative cross peaks at (25.5, 23.2) min and (23.2, 25.5) min arise from the coordinated decrease in the intensity of band A and simultaneous increase in intensity of band B [correlation (A↔B)] [2, 3]. Furthermore, the negative cross peaks at (25.5, 22.5) min and (22.5, 25.5) min come from the coordinated decrease in intensity of band A and simultaneous increase in intensity of band C. These correlations clearly imply the existence of coherent variation in GPC trace intensities at these elution times, and are reflected in CSq_1 and CSq_2. Comparison of the relative intensities of the A and B autopeaks shows the former to be more intense. This fact indicates that dynamic variation in concentration of the monomers [probably via hydrolysis of TESi-PS (2400)] makes a major contribution to step I.

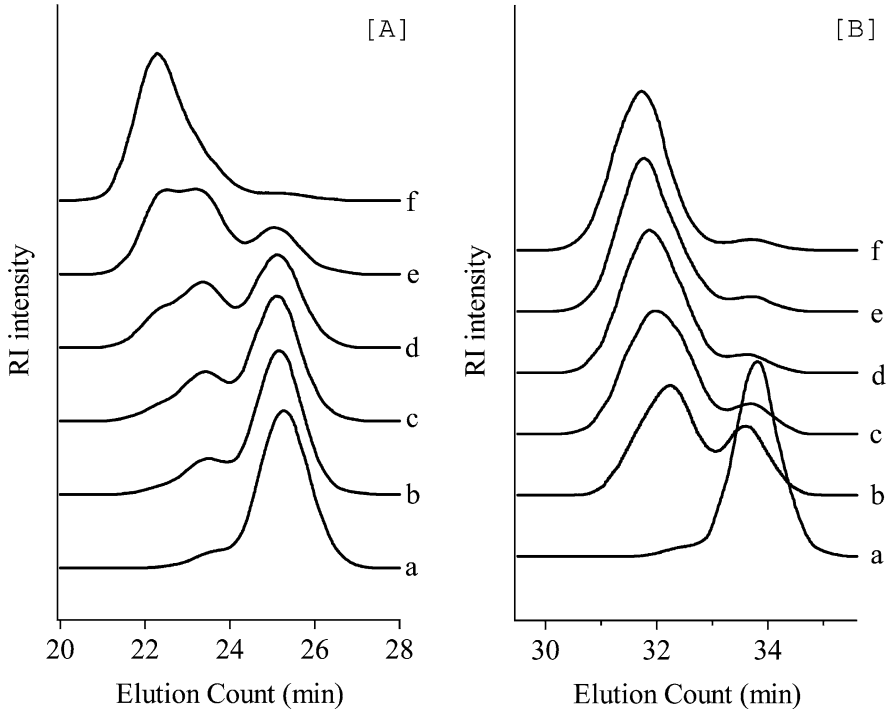

Fig. 2[A],[B] Time-resolved gel-permeation chromatography elution profiles of the CH_3SO_3H-catalyzed **[A]** TESi-PS (2400)–THF and **[B]** TESi-PS (8000)–THF systems. *a* $t = 0$ h, *b* $t = 0.5$ h, *c* $t = 1$ h, *d* $t = 2$ h, *e* $t = 4$ h, *f* $t = 24$ h. *RI* Refractive index

Table 1 Tentative assignment of elution peaks in time-resolved GPC spectra of TESi-PS (2400)–THF and TESi-PS (8000)–THF

	Conventional GPC		2D GPC		Assignment
	Counts (min)	Band no.	Counts (min)[a]	Band no.[b]	
TESi-PS (2400)			25.6–26.1	A_H	THSi-PS (2400) (hydrolyzed monomer)
	25.3	A	25.0–25.5	A	TESi-PS (2400) (monomer)
			24.6–24.7	A_L	Solvated monomer
	23.4	B	23.0–23.5	B	Dimer
	22.3	C	22.0–22.5	C	Trimer
			21.5–21.6	D	Tetramer
TESi-PS (8000)	33.8	A	33.7–33.9	A	TESi-PS (8000) (monomer)
			33.4–33.6	A_L	Solvated monomer
			32.7–32.9	B_H	Hydrolyzed dimer
	32.5	B	32.4–32.6	B	Dimer
			32.1–32.3	B_L	Solvated dimer
	31.6	C	31.5–31.7	C	Trimer
			31.2–31.4	C_L	
			30.9–31.1	D	Tetramer
			30.5–30.7	E	Pentamer

[a]The errors of elution peaks are ± 0.1 min
[b]Subscript H = high elution component; subscript L = low elution component

In the asynchronous spectrum (step I) of TESi-PS (2400) (Fig. 3b), we find that band A is made up of at least two bands at (25.6–26.1, 24.9–25.1) min and (25.6–25.8, 24.6–24.7) min fused together. Previously, the multiple components A_H, A and A_L of band A had been detected by the resolution enhancing characteristics of the 2D GPC spectra [2, 3]. The positive cross peaks arising from the $A_H \leftrightarrow A$ and $A_H \leftrightarrow A_L$ correlations indicate that the A_H component changes first, followed by change in the A or A_L component [2, 3]. Component A_H correlates with components B and C, furnishing the negative cross peak extending in the region $E_1 = 25.3$–26.6 min and $E_2 = 21.5$–24.0 min. The A and A_L components correlate with component B, resulting in the positive cross peaks at (24.9–25.0, 23.4) min and (24.6, 23.4) min, respectively. The appearance of the positive cross peak at (23.4, 22.4) min indicates a $B \leftrightarrow C$ correlation, with the dimer (band B) changing first followed by the trimer (band C). The order of other events is listed in Table 3. It should be noted that in step I both components B (dimer) and C (trimer) are produced rapidly as a consequence of consumption of components A_H, A and A_L.

In the synchronous map (step II) of TESi-PS (2400) (Fig. 4a), the $A \leftrightarrow C$ correlation furnishes two autopeaks and two negative cross peaks which together construct a correlation square (CSq_3). Since we may assume that a very weak autopeak coming from the B component exists at circa 23.7 min [2, 3], we may then construct a weak correlation square CSq_4 by connecting the autopeaks B and C with the two negative cross peaks at (25.1, 22.2) min and (22.2, 25.1) min. However, consideration of the relative intensities of the three autopeaks leads to the conclusion that the $A \leftrightarrow C$ correlation contributes to a major extent to step II, and that an increase in the population of C occurs rapidly in this step.

In the asynchronous map (step II) of TESi-PS (2400) (Fig. 4b), the correlations of band A with bands B and C leads to the positive and negative cross peaks at (25.2, 23.4) min and (25.2, 21.9) min, respectively. The result implies that the A components are consumed to produce the B and C components. The strong correlation of band B with band C provides the positive cross peak at (23.4, 22.3) min, which arises from the simultaneous production of the C component and consumption of the B component.

TESi-PS (8000)

The synchronous spectrum (step I) for TESi-PS (8000) is shown in Fig. 5a. The $A \leftrightarrow C$ correlation furnishes two autopeaks and two negative cross peaks, which define the correlation square CSq_1 (Table 2), reflecting the existence of coherent variation of GPC intensities at these elution times. The very strong intensity of autopeak A at 33.9 min implies that hydrolysis of the TESi-PS (8000) monomers occurs rapidly, in step I, to produce the trimer (band B).

In the asynchronous spectrum (step I) of TESi-PS (8000) (Fig. 5b), the positive cross peak at (33.9, 33.4) min indicates that band A consists of components A and A_L. Correlation of component A_L with band B provides the positive cross peak at (33.6, 32.4) min, indicating that the B component changes first and change in the A_L component follows [2, 3]. The $A \leftrightarrow C$ correlation furnishes the negative cross peak at (33.9, 31.5–31.7) min, implying that the C component changes

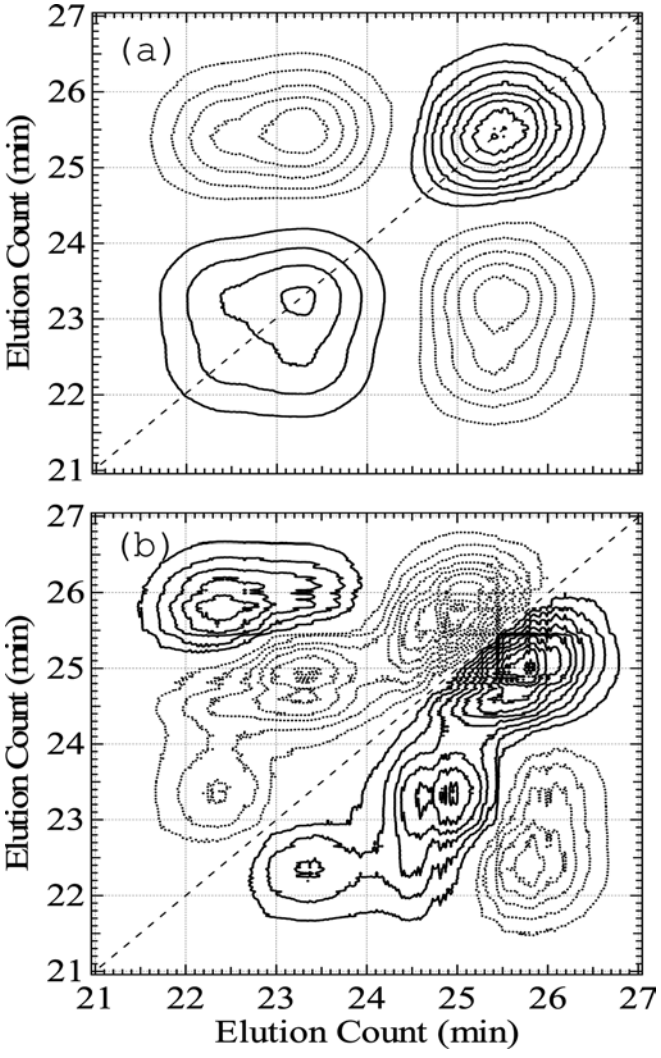

Fig. 3a, b Synchronous (**a**) and asynchronous (**b**) spectra of step I (0, 0.5, 1, 2 h) CH_3SO_3H-catalyzed TESi-PS (2400)-THF system

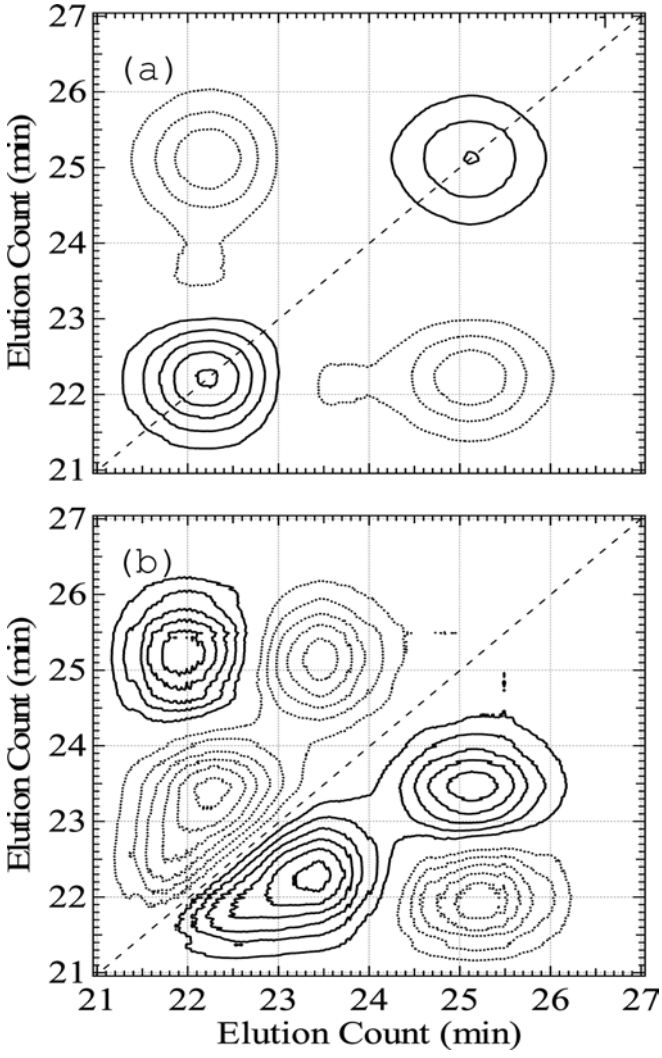

Fig. 4a, b Synchronous (**a**) and asynchronous (**b**) spectra of step II (2, 4, 24 h) for the CH_3SO_3H-catalyzed TESi-PS (2400)-THF system

first followed by the A component. The strong positive cross peak at (32.4, 31.7) min, arising from the B↔C correlation, indicates that consumption of the B component is followed by rapid production of the C components.

The synchronous spectrum (step II) for TESi-PS (8000) is shown in Fig. 6a. The B↔C correlation provides two autopeaks and two negative cross peaks which together define a correlation square CSq_2 (Table 2). Since the intensities of these four peaks are very strong, the B↔C correlation is the dominant contributor to step II. In other words, consumption of the dimers (band B) occurs rapidly to produce trimers (band C). The very weak correlation squares CSq_3 and CSq_4 suggest that although the A↔B and A↔D correlations exist, they do so to only a very small extent.

In the asynchronous spectrum (step II) of TESi-PS (8000) (Fig. 6b), we find that band B consists of components B_H, B and B_L, providing the negative cross peak in the region $E_1 = 32.0$–33.0 min and $E_2 = 30.0$–33.0 min. Correlations of the B_H and B components with band C yield the two positive, fused cross peaks at (32.4–32.8, 31.7) min. The positive cross peak at (32.9, 31.4) min arises from the B_H↔C correlation. These three components correlate with bands C and D, rendering the region consisting of negative cross peaks. In particular, the correlation of component B_L with bands C and D brings about the very strong negative cross peaks. Furthermore, the contour level of this region extends to $E_2 = 30.5$ min, showing that the B_L component correlates with the pentamers (band E), although to only a very small extent. It should be noted that band C consists of components C and C_L, which are seen in the very strong positive cross peak at (31.7, 31.3) min. The correlation of component C with band D appears as a very

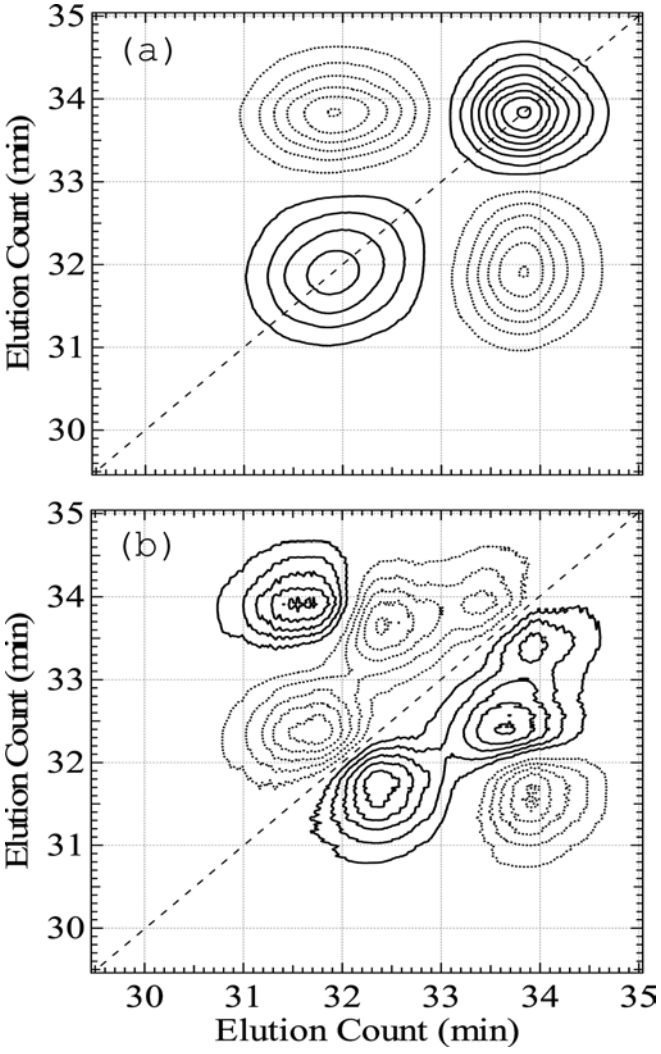

Fig. 5a, b Synchronous (**a**) and asynchronous (**b**) spectra of step I (0, 0.5, 1, 2 h) for the CH_3SO_3H-catalyzed TESi-PS (8000)-THF system

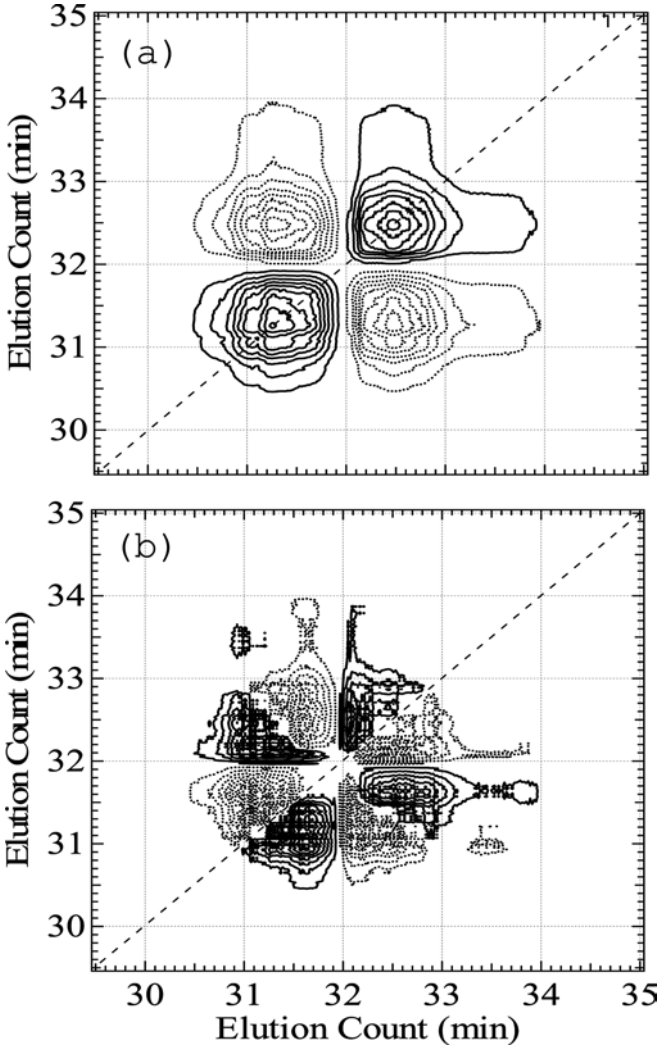

Fig. 6a, b Synchronous (**a**) and asynchronous (**b**) spectra of step II (2, 4, 24 h) for the CH_3SO_3H-catalyzed TESi-PS (8000)-THF system

strong positive cross peak at (31.7, 31.0) min. Moreover, component C_L correlates with band D, resulting in the appearance of an extremely strong positive cross peak at (31.3, 31.2) min. There also exists a very weak positive correlation between bands C (trimer) and E (pentamer) at circa (31.6, 30.6) min.

The difference in band correlations between the synchronous and asynchronous maps of TESi-PS (2400) with those of TESi-PS (8000) may be summarized as follows.

Step I (a) synchronous behaviors For TESi-PS (2400), A (monomer)↔B (dimer) and A (monomer)↔C (trimer) correlations coexist. The difference in the height of the contour levels suggests that the extent of the former correlation is slightly larger than that of the latter. Conversely, for TESi-PS (8000), it is the A (monomer)↔C (trimer) correlation which is predominant.

Table 2 Possible synchronous correlation squares (CSq_i: $i = 1$–5) and band correlations for the CH_3SO_3H-catalyzed TESi-PS (2400)–THF and TESi-PS (8000)–THF systems

	Step	CSq_i	Band Correlations
TESi-PS (2400)–THF	I	CSq_1	A↔B
		CSq_2	A↔C
	II	CSq_3	A↔C
		(CSq_4)	(B↔C)[a]
TESi-PS (8000)–THF	I	CSq_1	A↔C
	II	CSq_2	B↔C
		(CSq_3)	(A↔B)[a]
		(CSq_4)	(A↔D)[a]
		(CSq_5)	(B↔D)[a]

[a]Very weak

Step I (b) asynchronous behaviors For TESi-PS (2400), the asynchronous map provides direct evidence for the existence of components A_H, A and A_L, which correlate with bands B (dimer) and C (trimer). In particular, the intensities of the positive cross peaks for TESi-PS (2400), in the region $E_1 = 25.0$–27.0 min and $E_2 = 24.3$–26.0 min, which arise from correlations between A_H, A and A_L, are extremely strong. Conversely, for TESi-PS (8000), the band intensity coming from the monomeric components in the regions $E_1 = 33.0$–35.0 min and $E_2 = 33.0$–34.0 min is weak, while the B↔C correlation is strong compared with that in the TESi-PS (2400) system.

Step II (a) synchronous behaviors For TESi-PS (2400), the A↔C correlation is predominant, while the extent of the B↔C correlation is very small. Conversely, for TESi-PS (8000), the B↔C correlation is extremely strong, although very weak A↔B and A↔C correlations coexist.

Step II (b) asynchronous behaviors For the TESi-PS (2400) system, three relatively strong correlations, A↔B, A↔C and B↔C, coexist with the B↔C correlation being of slightly stronger extent. For the TESi-PS (8000) system, the asynchronous map indicates directly the existence of components B_H, B and B_L and C and C_L. The B_H, B and B_L components correlate with bands C and D, which arise from formation of trimers and tetramers. The components C_L and C are consumed to produce tetramers (band D) and pentamers (band E). Thus, for TESi-PS (8000) in step II, the correlations B_H, B, B_L↔C, D; C_L↔D and C↔E are predominant.

We observe that the two sample systems provide a marked difference in the synchronous and asynchronous behaviors between the two steps. The A_H and A_L components, which appear in the asynchronous map (step I) for TESi-PS (2400), may be assigned to the hydrolyzed or partially hydrolyzed monomers (THSi-PS) and the THF-solvated THSi-PS monomers [7], respectively. For TESi-PS (2400), the correlations of band A and its components with bands B and C are generally predominant in the synchronous and asynchronous maps throughout steps I and II. In particular, the strong correlation of the A_H, A and A_L components with bands B and C in step I may imply an increased population of condensates B and C as components A_H, A, and A_L are consumed. We note the existence of components B_H, B and B_L in step II for the TESi-PS (8000) system. The B_H and B_L components may be assigned to the hydrolyzed or partially hydrolyzed dimers and their solvated species [7]. It is evident that the correlations of components B_H, B and B_L with components C, C_L, D and E are predominant in step II, implying that formation of these species plays a critical role in the growth of longer oligomers. We address this factor in the following discussion of the reactivity of the components.

The B_H component correlates mainly with bands C and C_L. The B_H↔C correlation is strong, while the B_H↔C_L correlation is only moderate (Table 3). Moreover, the B_H↔D correlation is very weak, and there is no evidence for a B_H↔E correlation. Conversely, the B and B_L components correlate strongly not only with the C and C_L bands, but also with band D, and the B and B_L components correlate only weakly with band E. This result implies that, compared with the B and B_L species, the B_H species is more reactive and rapidly consumed to form longer oligomers. The difference in the extent of correlation among the B_H, B and B_L components may arise from the differences in their reactivities. Similarly, component C correlates strongly with component D but weakly with component E, while although the C_L component correlates with that of D, it does not correlate with component E. The result implies that the latter component E is more reactive than component D.

A TESi-PS (2400) molecule is much less hydrophobic than a TESi-PS (8000) molecule, leading to the reduced extent of aggregation and increasing the population of TESi-PS (2400) molecules in the monomolecular state. This environment may promote an increased population of the A_H, A and A_L components, thereby strengthening the A_H, A B B, and C correlations. Conversely, since the greater hydrophobicity of TESi-PS (8000) promotes formation of aggregates, the population of the monomeric components may decrease, resulting in the reduced extent of the correlations of the monomeric components with those of B and C.

In our previous study [10], we showed that the TESi-PS dimer is reversibly hydrolyzed to provide monomeric TESi-PS, which can condense with a dimer to form a trimer. We may assume the following cascade steps in the polymerization process.

$$\text{Monomers(A)}[\leftarrow]\text{Monomers}(A_H \text{ or } A_L) \tag{6}$$

$$\text{Monomers}(A_H \text{ or } A_L) \rightleftarrows \text{Dimers(B)} \tag{7}$$

$$\text{Dimers}(B_H, \text{B or } B_L) + \text{Monomers}(A_H \text{ or } A_L)[\leftarrow]\text{Trimers(C or } C_L) \tag{8}$$

$$\text{Trimers(C)} + \text{Monomers}(A_H \text{ or } A_L)[\leftarrow]\text{Tetramers(D)} \tag{9}$$

The cascade steps shown in Eq. 8and Eq. 9, involving condensation between the monomeric species (A_H, A and A_L) and the dimeric (or trimeric) species, thereby increasing the correlations of the monomeric species with components B and D, lie well to the right.

The existence of components arising from hydrolysis or partial hydrolysis of ethoxysilyl groups may be possible for dimers and longer oligomers, since steric hindrance of the PS chain promotes probable isolation

Table 3 Synchronous and asynchronous band correlations, signs and order of events for the CH_3SO_3H-catalyzed TESi-PS (2400)-THF and TESi-PS (8000)-THF systems.*vs* Very strong, *s* strong, *m* medium, *w* weak, *vw* very weak

	Step	Correlation		Sign		Order of events[c,d]
				(Φ)[a]	(Ψ)[b]	
TESi-PS (2400)-THF	I	$A_H \leftrightarrow A$, A_L	s	+	+	$A_H \rightarrow A$, A_L
		$A_H \leftrightarrow B$	m	-	-	$A_H \rightarrow B$
		$A_H \leftrightarrow C$	s	-	-	$A_H \rightarrow C$
		A, $A_L \leftrightarrow B$	m	+	-	$B \rightarrow A$, A_L
		$B \leftrightarrow C$	m	+	+	$B \rightarrow C$
	II	$A \leftrightarrow B$	m	+	+	$A \rightarrow B$
		$A \leftrightarrow C$	s	-	-	$A \rightarrow C$
		$B \leftrightarrow C$	s	+	-	$C \rightarrow B$
TESi-PS (8000)-THF	I	$A \leftrightarrow A_L$	m	+	+	$A \rightarrow A_L$
		$A_L \leftrightarrow B$	s	+	-	$B \rightarrow A_L$
		$A \leftrightarrow C$	s	-	-	$A \rightarrow C$
		$B \leftrightarrow C$	s	+	+	$B \rightarrow C$
	II	$A \leftrightarrow C$	vw	-	+	$C \rightarrow A$
		$A_L \leftrightarrow D$	vw	-	-	$A_L \rightarrow D$
		$B_H \leftrightarrow B$	m	+	-	$B \rightarrow B_H$
		$B \leftrightarrow B_L$	vs	+	-	$B_L \rightarrow B$
		$B_H \leftrightarrow C$	s	-	+	$C \rightarrow B_H$
		$B_H \leftrightarrow C_L$	m	-	+	$C_L \rightarrow B_H$
		$B \leftrightarrow C$	vs	-	+	$C \rightarrow B$
		$B \leftrightarrow C_L$	w	-	+	$C_L \rightarrow B$
		$B \leftrightarrow D$	m	-	-	$B \rightarrow D$
		$B \leftrightarrow E$	m	-	-	$B \rightarrow E$
		$B_L \leftrightarrow C$, C_L, D	vs	-	-	$B_L \rightarrow C$, C_L, D
		$B_L \leftrightarrow E$	m	-	-	$B_L \rightarrow E$
		$C \leftrightarrow C_L$, D	vs	+	+	$C \rightarrow C_L$, D
		$C \leftrightarrow E$	s	+	+	$C \rightarrow E$
		$D \leftrightarrow E$	m	+	+	$D \rightarrow E$

[a]Synchronous
[b]Asynchronous
[c]$E_x \rightarrow E_y$; the event E_x occurs before E_y
[d]Subscripts *H* and *L* represent high and low elution components, respectively

of any ethoxysilyl groups which may be incorporated into the aggregates. This isolation effect may account for the difference in the extent of hydrolysis of the ethoxysilyl groups. The effect should be greater in the TESi-PS (8000) system than in the TESi-PS (2400) system, resulting in the observed difference in their respective reactivities.

We may postulate both linear and cyclic molecular structures for a dimeric species [Fig. 7a, b (I)]. However, since the TESi-PS dimer is reversibly hydrolyzed, we may assume a preference for a linear structure in the polymerization process. The steric hindrance caused by the bulky and rigid PS chains and their high hydrophobicity would induce a difference in the extent of hydrolysis of ethoxysilyl groups in a linear molecule [Fig. 7 (II)]. Hydrolyzed and partially hydrolyzed dimers and their solvated species probably give rise to bands B_H and B_L, respectively, and the unhydrolyzed species furnish band B.

In the TESi-PS (2400) system (steps I and II), which is less aggregated than the TESi-PS (8000) system, the cascade step shown in Eq. 6 probably lies in the direction of the long arrow, while the step shown in Eq. 7 lies toward the monomeric species, giving rise to the predominant correlations of components A_H, A and A_L with bands B and C. Consequently, interaction between a monomer and an oligomer is predominant throughout the two steps of the polymerization.

However, in the TESi-PS (8000) system (step II), aggregation may result in the predominant correlations of the B_H, B and B_L components with the longer oligomeric species (C, C_L, D and E). When the TESi-PS molecules form a reversed micelle-type aggregate in organic solvents, the triethoxy groups are concentrated in the polar core. The steric hindrance of the bulky and rigid PS chains and their high hydrophobicity probably induce formation of aggregate structures which are limited in size, and aggregation numbers N ($N = 2$, 3 and 4) will be predominant. Therefore, in addition to the dimer-longer oligomer correlations, correlations of the trimer (C and C_L) with the tetramer (D) and the pentamer (E) and, specifically, the D B E correlation, appear in step II for TESi-PS (8000). Therefore, we may assume the existence of following cascade steps, which become predominant in step II for this system.

$$\text{Dimer} + \text{Dimer}[\leftarrow]\text{Tetramer} \tag{10}$$

$$\text{Dimer} + \text{Trimer}[\leftarrow]\text{Pentamer} \tag{11}$$

Accordingly, in addition to the monomer-oligomer interactions, the interaction between oligomer and oligomer arising from the condensation reaction, becomes predominant in step II. Thus, the steps shown in Eq. 10 and Eq. 11 lie in the direction of the long arrow. For the tetramer and longer oligomers, co-existence of the reactive and less-reactive components may be possible.

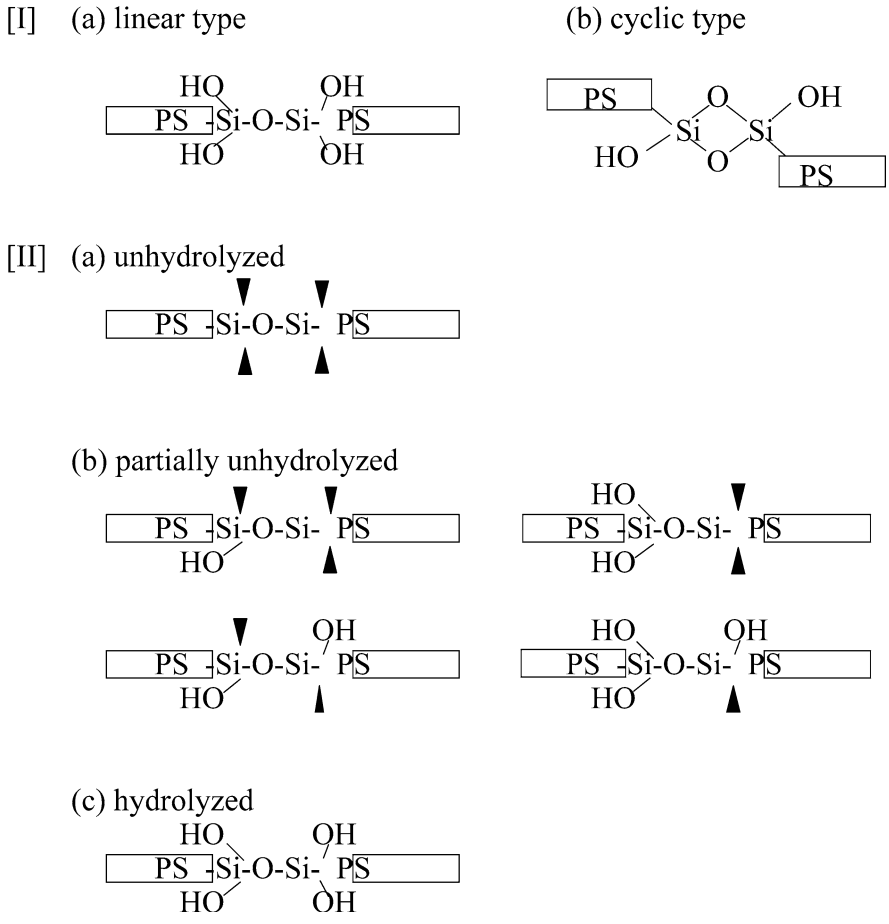

Fig. 7 Possible molecular structures (*I*) and (*II*) of the TESi-PS dimers. *PS* Polystyrene chain, *triangle* ethoxy group

Currently, it is difficult to detect such species even with the 2D GPC technique, since the difference in elution time of longer oligomers is vanishingly small.

The oligomer-oligomer interactions for TESi-PS arise not only from formation of a siloxane bond but also from the very hydrophobic PS chains. A hydrophobic interaction between oligomers should hinder elongation of a polymer via the chemical bond formation during polymerization. Therefore, the formation of oligomers with high reactivity may play a critical role in the elongation process. Recently, Stellbrink et al. [19] used small angle neutron scattering to demonstrate aggregational behavior of styryl lithium head groups in benzene. The result indicated that dimers and tetramers were produced in a first step before large-scale formation of self-assembled aggregates. However, very little is known about the significance of hydrophobic interactions between aggregates during polymerization. Since the reactivity of longer oligomers may be intrinsically correlated with their steric structures, further research along these lines is highly desirable.

Conclusion

The CH_3SO_3H-catalyzed polymerization process of the well-defined polymeric SCAs, triethoxysilyl-terminated polystyrenes, TESi-PS (2400) and TESi-PS (8000), which were used instead of simple SCAs with low molecular weight ($M_n < 1000$), has been examined by 2D GPC. A detailed discussion of oligomer–oligomer interactions became possible based on the explicit determination of molecular weight and assignment of each oligomeric aggregate. It was found that there exists a marked difference in the process of polymerization of TESi-PS (2400) and TESi-PS (8000), probably reflecting the difference in the extent of aggregation of these two triethoxysilyl-terminated polystyrene systems.

References

1. Noda I (1990) Appl Spectrosc 44:550
2. Noda I (1993) Appl Spectrosc 47:1329
3. Noda I, Dowrey AE, Marcott C, Story GM, Ozaki Y (2000) Appl Spectrosc 54:236A
4. Izawa K, Ogasawara T, Masuda H, Okabayashi H, Noda I (2001) PhysChemComm 12:1
5. Izawa K, Ogasawara T, Masuda H, Okabayashi H, O'Connor CJ, Noda I (2002) PhysChemComm 2:1
6. Izawa K, Ogasawara T, Masuda H, Okabayashi H, Noda I (2002) Macromolecules 35:92
7. Izawa K, Ogasawara T, Masuda H, Okabayashi H, O'Connor CJ, Noda I (2002) Phys Chem Chem Phys 4:1053
8. Izawa K, Ogasawara T, Masuda H, Okabayashi H, O'Connor CJ, Noda I (2002) J Phys Chem B 106:2867
9. Takaki M, Suzuki K, Mano T (1991) Koubunshi Ronbunshu 48:171
10. Takaki M, Suzuki K, Kondo Y, Oku J (1991) Polym J 23:917
11. Suzuki K, Esaki M, Misawa A, Takaki M (1994) Koubunshi Ronbunshu 51:11
12. Suzuki K, Oku J, Okabayashi H, O'Connor CJ (2003) Langmuir 19:7611
13. Munir A, Goethals EJ (1981) Makromol Chem Rapid Commun 2:693
14. Lee KW, MacCarthy TJ (1988) Macromolecules 21:3353
15. Sander LM (1987) Sci Am 256:94
16. Ogasawara T, Nara A, Okabayashi H, Nishio E, O'Connor CJ (2000) Colloid Polym Soc 278:1070
17. Izawa K, Ogasawara T, Masuda H, Okabayashi H, Monkenbnsch M, O'Connor CJ (2002) Colloid Polym Soc 280:725
18. Suzuki K, Oku J, Okabayashi H, O'Connor CJ (2003) Polym J 35:938
19. Stellbrink J, Willner L, Jucknischke O, Richter D, Lindner P, Fetters LJ, Huang JS (1998) Macromolecules 31:4189